JARO

ORIGINAL ARTICLE: GENERAL RESEARCH

Distortion Product Otoacoustic Emissions in Mice Above and Below the Eliciting Primaries

Mary Ann Cheatham[1] 🔘

Abstract

Normal hearing is associated with cochlear nonlinearity. When two tones (f1 and f2) are presented, the intracochlear response contains additional components that can be recorded from the ear canal as distortion product otoacoustic emissions (DPOAEs). Although the most prominent intermodulation distortion component is at 2f1-f2, other cubic distortion products are also generated. Because these measurements are noninvasive, they are used in humans and in animal models to detect hearing loss. This study evaluated how loss of sensitivity affects DPOAEs with frequencies above and below the stimulating primaries, i.e., for upper sideband (USB) components like 2f2-f1 and for lower sideband (LSB) components like 2f1-f2. DPOAEs were recorded in several mouse mutants with varying degrees of hearing loss associated with structural changes to the tectorial membrane (TM), or with loss of outer hair cell (OHC) somatic electromotility due to lack of prestin or to the expression of a non-functional prestin. In mice with changes in sensitivity, magnitude reductions were observed for 2f1-f2 relative to controls with mice lacking prestin showing the greatest changes. In contrast, 2f2-f1 was minimally affected by reductions in cochlear gain due to changes in the TM or by the loss of OHC somatic electromotility. In addition, TM mutants with spontaneous otoacoustic emissions (SOAEs) generated larger responses than controls at 2f2-f1 when its frequency was similar to that for the SOAEs. Although cochlear pathologies appear to affect USB and LSB DPOAEs in different ways, both 2f1-f2 and 2f2-f1 reflect nonlinearities associated with the transducer channels. However, in mice, the component at 2f2-f1 does not appear to receive enhancement due to prestin's motor action.

Keywords Intermodulation distortion · Mutant mice · Otoacoustic emissions · Prestin · Tectorial membrane

Introduction

Otoacoustic emissions are clinically important as they serve to separate cochlear from retro-cochlear disorders. Hence, they can assist in the differential diagnosis of sensory changes associated with the active processes linked to outer hair cells (OHCs). Given the original suggestion [1] that distortion product otoacoustic emissions (DPOAEs) can consist of a combination of two emission sources, as well as the controversy over how they travel to the ear canal [2], analysis of DPOAEs in mutants with different pathologies is warranted. In addition to mice lacking prestin or expressing a nonfunctional prestin, mice with genetic deletions

or mutations affecting the tectorial membrane (TM) were studied. Previous work in rabbits exposed to noise showed increases at 2f2-f1 even when 2f1-f2 decreased [3]. This differential sensitivity to insult prompted the comparison of upper sideband (USB, 2f2-f1) and lower sideband (LSB, 2f1-f2) DPOAEs in mouse models with varying degrees of hearing loss.

High levels of prestin protein are expressed in the OHC's lateral membrane, providing the molecular basis for somatic electromotility [4]. Animals lacking prestin or expressing non-functional prestin [5], have an approximately 50 dB threshold shift [6] and broad tuning [7], similar to changes created by loss of OHCs [8–10] or by detachment of the TM from the organ of Corti [11]. However, at high stimulus levels, prestin knockout (KO) mice generate DPOAEs [12] that disappear post mortem. The latter are thought to reflect operation of the mechanoelectrical transducer (MET) channels associated with hair bundle mechanical properties [13]. In contrast to mice lacking prestin, TM mouse models of hereditary deafness

✉ Mary Ann Cheatham
  m-cheatham@northwestern.edu

[1] The Knowles Hearing Center, Roxelyn and Richard Pepper Department of Communication Sciences and Disorders, Northwestern University, 2-240 Frances Searle Building, 2240 Campus Drive, Evanston, IL 60208, USA

can retain near-normal hearing when young or can show varying degrees of hearing loss. In addition, these mutants are likely to generate spontaneous emissions (SOAEs) when threshold shifts are less than ~ 25 dB SPL [14]. This phenotype is unusual as normal mice and several other laboratory animals are rarely spontaneous emitters.

The TM is an extracellular component of the cochlea required for normal hearing [15]. It contains collagen fibrils embedded in a laminated, striated sheet matrix composed of TECTA, TECTB and CEACAM16. In contrast to mice lacking *Tecta* and *Tectb*, auditory brainstem responses (ABRs) and distortion production otoacoustic emissions are near normal in young *Ceacam16* null mutants on the C57BL6 background [16]. In this mouse model, the striated sheet matrix fails to form and approximately 70% of the mutants generate SOAEs compared to wildtype (WT) mice where approximately 6% are spontaneous emitters. Additional experiments revealed that mice heterozygous for a missense mutation in *Tecta* ($Tecta^{Y1870C+/-}$) also produced SOAEs even though they had hearing loss [17]. In these animals, Kimura's membrane becomes delaminated in basal regions of the cochlea and the subtectorial space increases [18]. The latter change is thought to elevate the ABRs to a greater degree than the emissions associated with OHC function. Hence, the ABR threshold shifts were ~ 50 dB SPL across frequency [17, 18]. Finally, in mice lacking *Tectb,* large reductions in sensitivity were observed for frequencies below ~ 25 kHz. However, at higher frequencies, the DPOAE thresholds were shifted by only about 15 dB SPL. In this mouse model, the striated sheet matrix does not develop, and the thickness and cross-sectional area of the TM increases dramatically in the apical half of the cochlea where large threshold shifts are recorded [19]. Although these mutants generate SOAEs, the incidence is only slightly higher than in controls and SOAE frequencies coincide with high-frequency regions where some degree of amplification is retained [14].

Threshold shifts were determined in these various mouse models for cubic intermodulation-distortion (IMD) components below f1 at 2f1-f2 and above f2 at 2f2-f1 to assay the degree to which the loss of sensitivity affected LSB and USB DPOAEs. Measurements from prestin knockout (KO, $Slc26a5^{-/-}$) and 499 prestin knockin (KI, $Slc26a5^{V499G/Y501H}$) [5] mice, as well as recordings from various mutants with TM defects ($Ceacam16^{-/-}$, $Tecta^{Y1870C+/-}$, $Tectb^{-/-}$), were compared to those from WT controls. The data demonstrate that 2f2-f1 is much smaller than 2f1-f2 in WT controls. In mouse mutants with partial loss of gain, and even in mice lacking prestin, the DPOAE at 2f2-f1 is comparable to controls. Finally, in TM mutants producing SOAEs, DPOAEs at 2f2-f1 can be enhanced relative to controls when their frequencies are similar to those for the SOAEs.

Materials and Methods

Animals were bred on site and data were acquired for both male and female mice on a C57BL6 (*Ceacam16*) or a mixed, variable 129/C57BL6 background. All procedures were approved by the Institutional Animal Care and Use Committee at Northwestern University, as well as by NIDCD.

Otoacoustic emissions (OAEs) were acquired under general anaesthesia (100 mg/kg ketamine and 10 mg/kg xylazine) in a sound isolation chamber using a custom probe designed and fabricated by J.H. Siegel. Results were acquired using SysRes [20] and EMAV [21], and with a Card Deluxe 24-bit sound card and a sampling rate of 96 kHz. Young mice (3–11 weeks of age) lacking prestin or expressing a non-functional mutated prestin, as well as mice with deletions or mutations in genes that affect the TM, were tested using DPOAEs to estimate changes in cochlear gain. Magnitudes of 2f1-f2 (LSB) and 2f2-f1 (USB) were compared to evaluate the effect of hearing loss on these two intermodulation distortion products in mutants with and without SOAEs. Both iso-input and input-output or growth functions were collected at various f2 frequencies. The level of f1 that produced a 2f1-f2 or a 2f2-f1 of 0 dB SPL was designated as threshold. It is also emphasized that the frequency ratio, f2/f1, was 1.2 for all measurements. Distortion in the sound was documented using a tubing coupler with a volume approximating that of the mouse ear canal with emission probe inserted. These results are referred to as coupler measurements and included in plots of the DPOAE input-output functions. Spectral averaging in the absence of stimulation was used to acquire SOAEs. A fast Fourier transform of the time waveform was performed and smoothed before integrating energy into windows of 93 Hz. It is also acknowledged that other stimulus paradigms, such as using a variable frequency ratio, might have provided additional insights into the differences between IMD products above and below the primaries. However, the observations were acquired over many years for various mouse models using our standard testing procedures. In addition, phase data are not available for any of the measurements.

Statistical analyses were performed in GraphPad Prism (San Diego CA) where a one-way analysis of variance (ANOVA) was executed followed by Tukey's multiple comparisons tests to obtain adjusted *p*-values. Tukey's was chosen when multiple data sets, mutants with and without SOAEs, were compared with a single control variable, the WT data. There were conditions, however, where only two data groups were compared and in these instances the Student's t-test (two-tailed distribution) was utilized, i.e., in Fig. 1 for the 70 dB SPL condition, and in Table 1 and Fig. 8 for the DPOAE thresholds obtained in mice lacking

Ceacam16 and their controls. Asterisks are used in the figures to designate statistical significance and the legends describe the statistical tests involved. Variability was designated using standard errors of the mean (SEM) for the DPOAE data and standard deviations (SD) for the SOAE frequencies, except for *Tectb*$^{-/-}$ where the full range of SOAE frequencies is provided. Methodological details are specified in previous publications [16, 17].

Fig. 1 Iso-input functions for adolescent *Ceacam16*$^{-/-}$ mice and their controls. Average DPOAE magnitudes (±SEM) for 2f1-f2 (panel **a**) are plotted as a function of the f2 frequency. The two primaries were presented at L1=L2=70 dB SPL (solid lines) or at L1=50 L2=35 dB SPL (broken lines). WT data are black, those for the mutants are red. Mutants generating SOAEs are plotted with dashed lines (n=30) for the DP gram obtained at L1=50 L2=35 dB SPL. Data for mutants without SOAEs are plotted with dot-dashed lines (n=22). Responses for the LSB DPOAE at 2f1-f2 were not statistically different for WT and *Ceacam16*$^{-/-}$ with SOAEs. However, mice lacking *Ceacam16* and lacking SOAEs were statistically different from WT at the f2 frequencies indicated by the asterisks ($p < 0.03$). The statistical analysis was performed using ANOVA followed by Tukey's multiple comparisons tests to obtain adjusted *p* values for each individual primary pair. For iso-input functions collected at L1=L2=70 dB SPL, SOAEs were documented in only 5 of the 19 mice lacking *Ceacam16*. Of the other 14 animals, some were probably not spontaneous emitters as no search was made for SOAEs and only 70% of *Ceacam16*$^{-/-}$ mice have SOAEs. In panel **b**, average magnitudes (±SEM) for the DPOAE at 2f2-f1 (L1=L2=70 dB SPL) are plotted at the f2 frequency. In panel **c**, 2f2-f1 is replotted as a function of the DPOAE frequency, i.e., at 2f2-f1. The average (±SD) SOAE frequency is designated along the abscissa by the horizontal arrow. Asterisks in panel **c** indicate statistical significance (Student's t-test, $p < 0.02$)
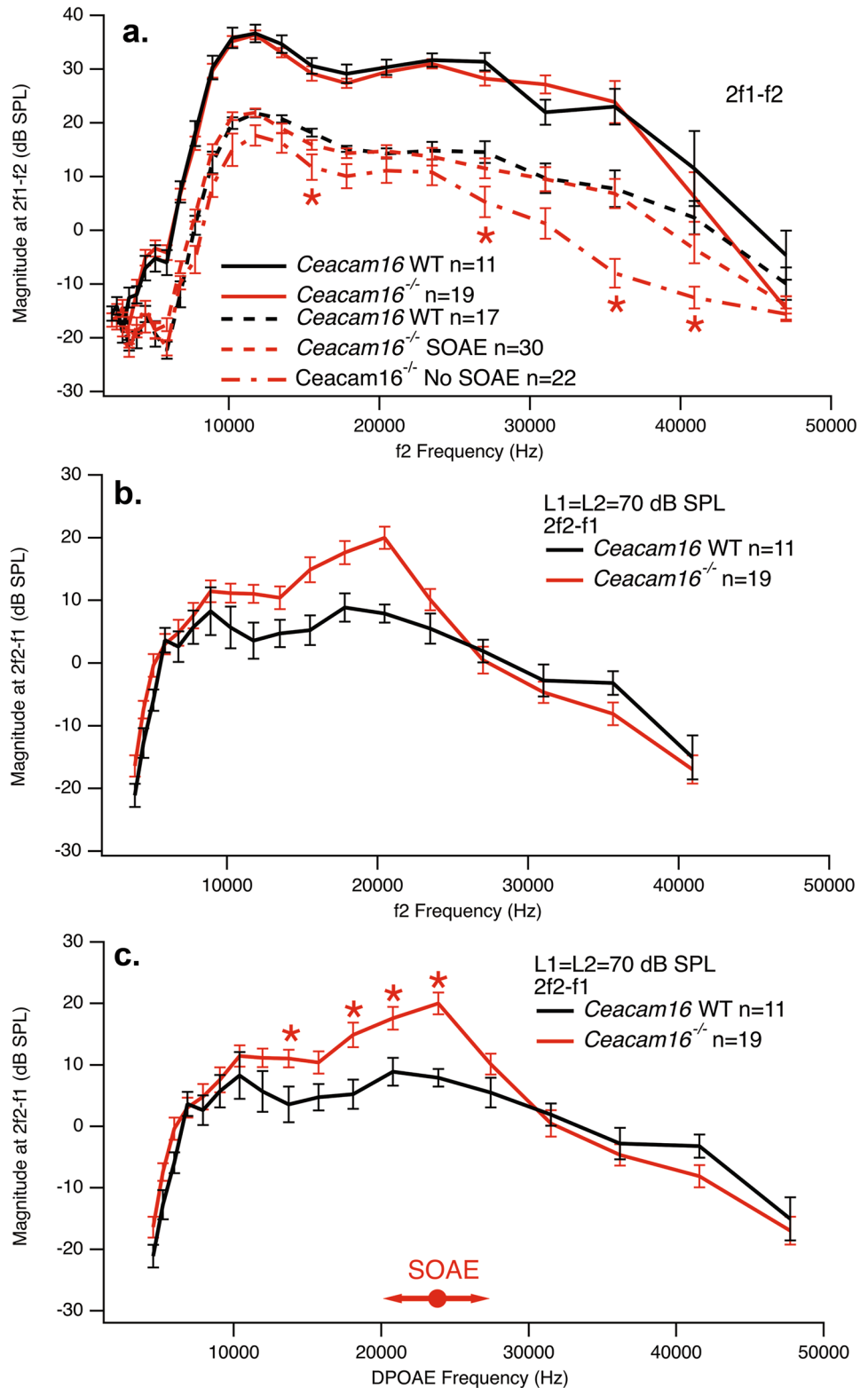
Results

Ceacam16⁻ᐟ⁻ **Mice**

DPOAE iso-input functions demonstrate that young mice lacking *Ceacam16* retain near-normal hearing consistent with their WT-like ABR thresholds [16]. Our previous data also indicated that 70% of null mutants generate SOAEs with an average frequency ($\pm$ SD) of 23.8 $\pm$ 3.7 kHz. Although only about 6% of WT controls independent of strain background are spontaneous emitters, their SOAEs present in a similar frequency region (average SOAE frequency $\pm$ SD = 22.6 $\pm$ 3.8 kHz). Figure 1a shows iso-input

Fig. 3 Iso-input functions for *Tecta^{Y1870C+/−}* mice and their controls. ▶ Data for 2f1-f2 are plotted as a function of the f2 frequency in panel **a**. Mutants with SOAEs (green solid lines) produce larger responses than mutants without SOAEs (green dashed lines). The DPOAE at 2f2-f1 is plotted as a function of the f2 frequency in panel **b** and shows larger responses in mutants with SOAEs. In panel **c**, 2f2-f1 is replotted as a function of the DPOAE frequency. The horizontal bar above the abscissa indicates the average SOAE frequency $\pm$ SD (15.4 $\pm$ 7.0 kHz)

functions or DP grams for L1 = L2 = 70 dB SPL (solid lines) and for L1 = 50 L2 = 35 dB SPL (broken lines). It is emphasized that only 5 of 19 mice were tested for SOAEs when the DP grams were collected at 70 dB SPL. No search for

Fig. 2 Iso-input functions for *Ceacam16⁻ᐟ⁻* mice and their controls at ~7 months of age. Average ($\pm$ SEM) DPOAE magnitudes are plotted as a function of f2 for 2f1-f2 in panel **a** and for 2f2-f1 in panel **b**. Primaries were presented at 70 dB SPL. At this age, these seven mutants did not generate SOAEs and the magnitudes for both USB and LSB emissions were reduced relative to controls
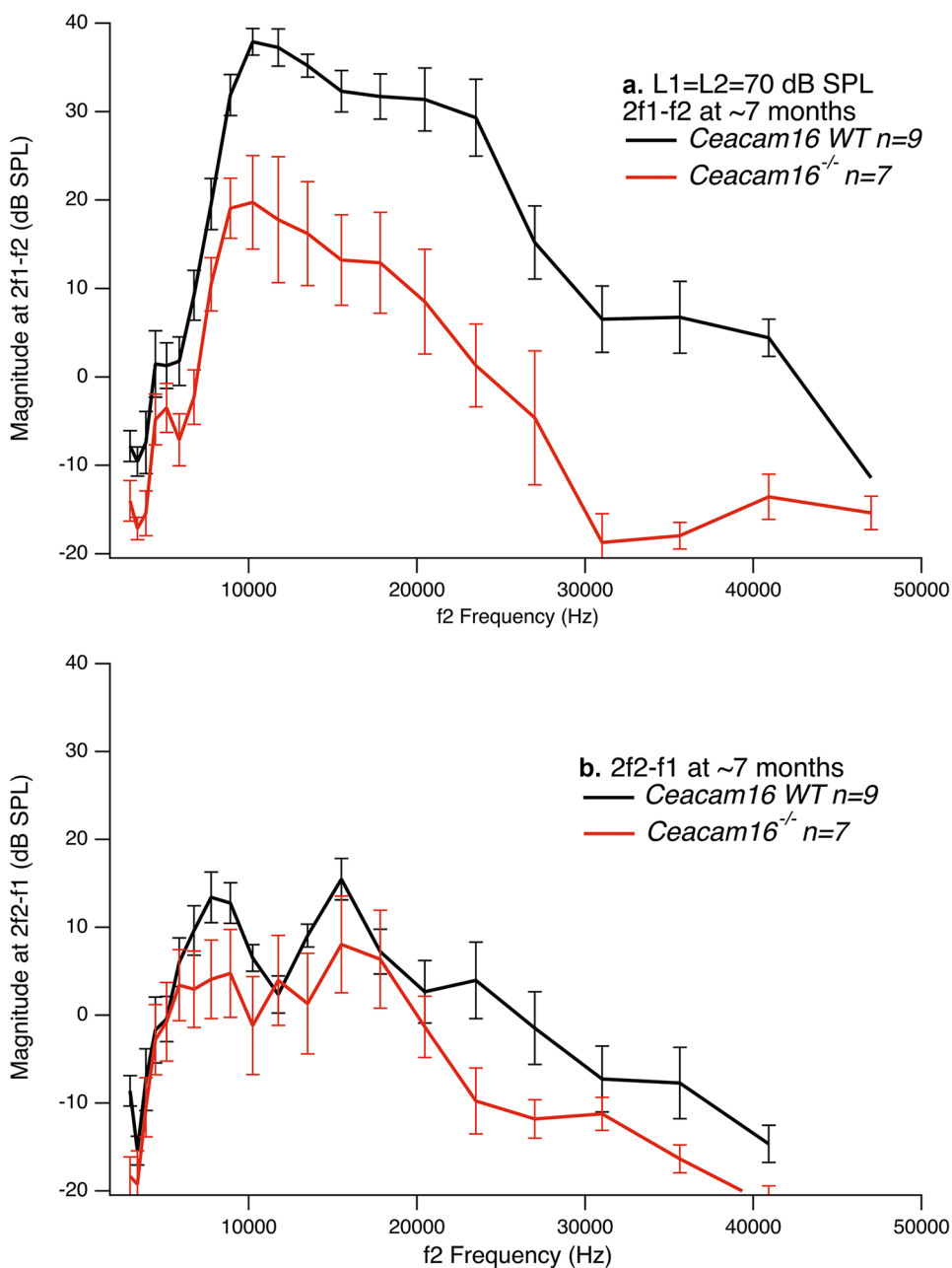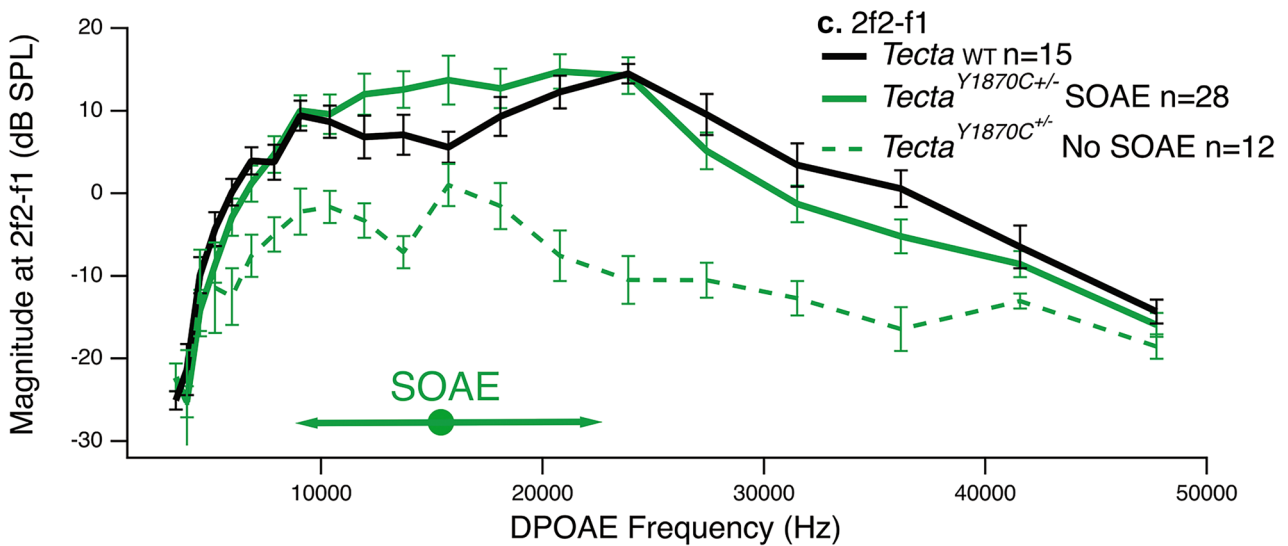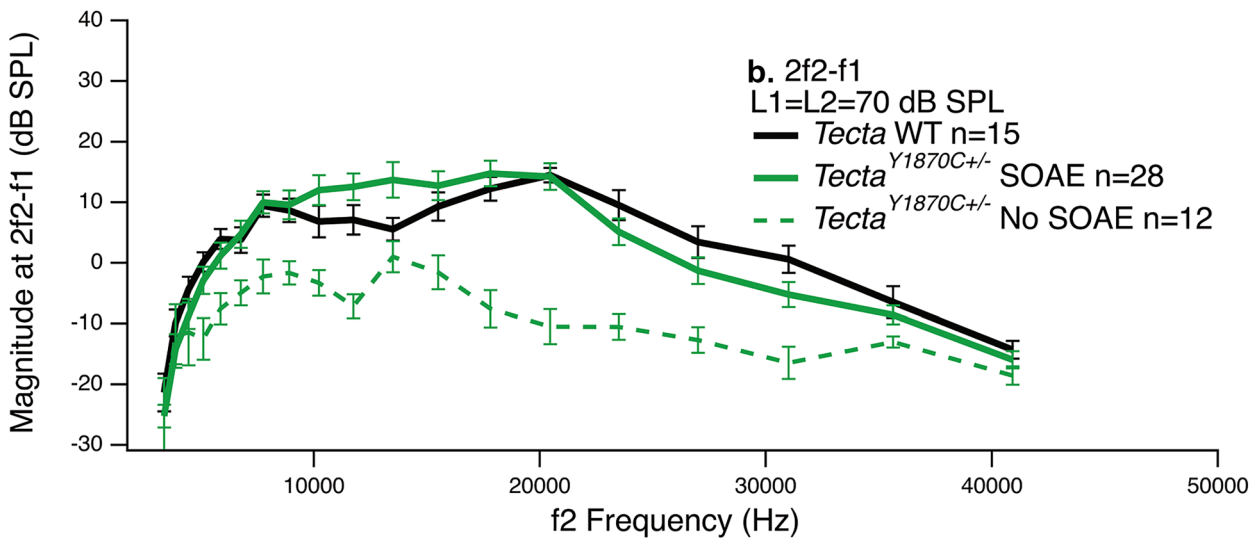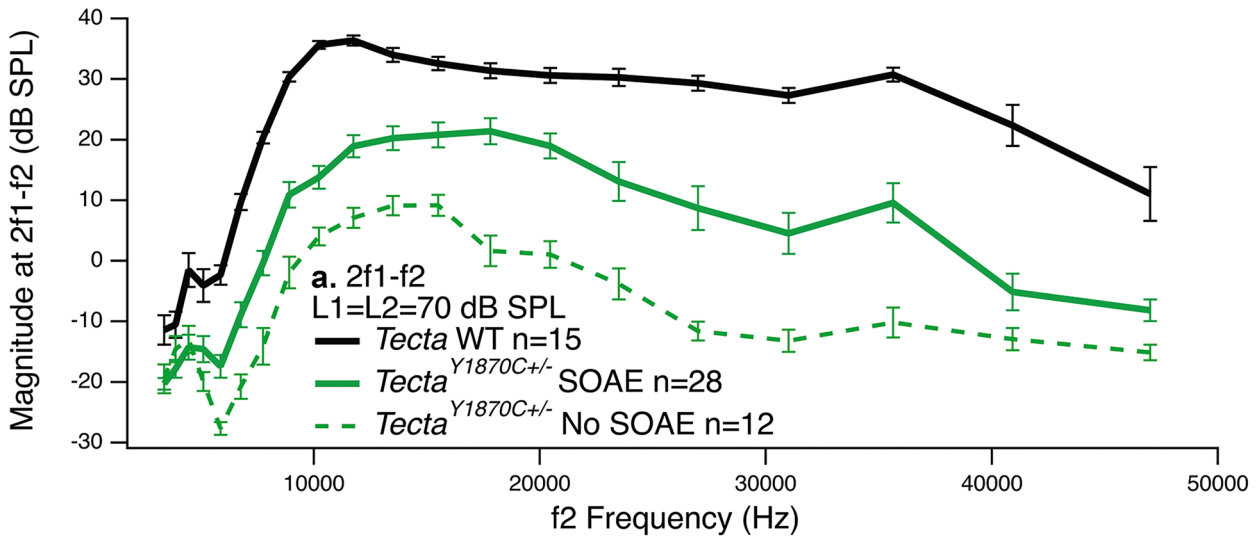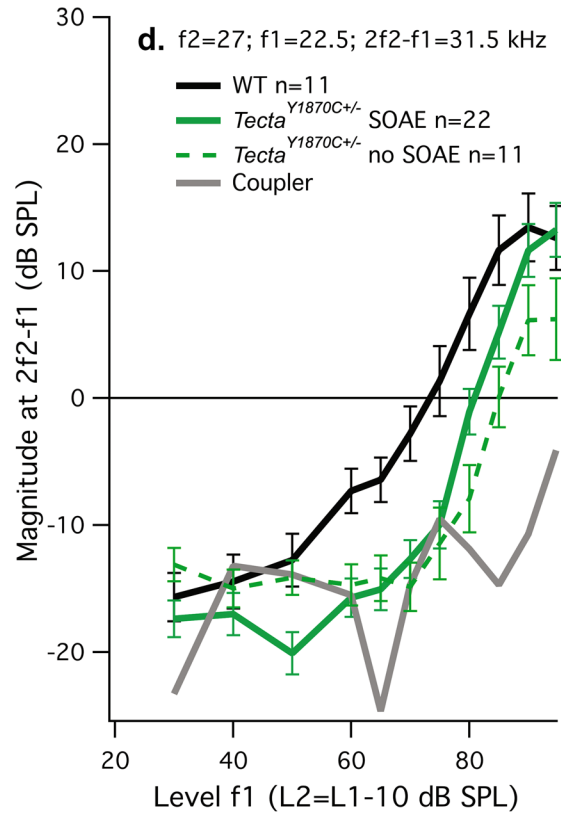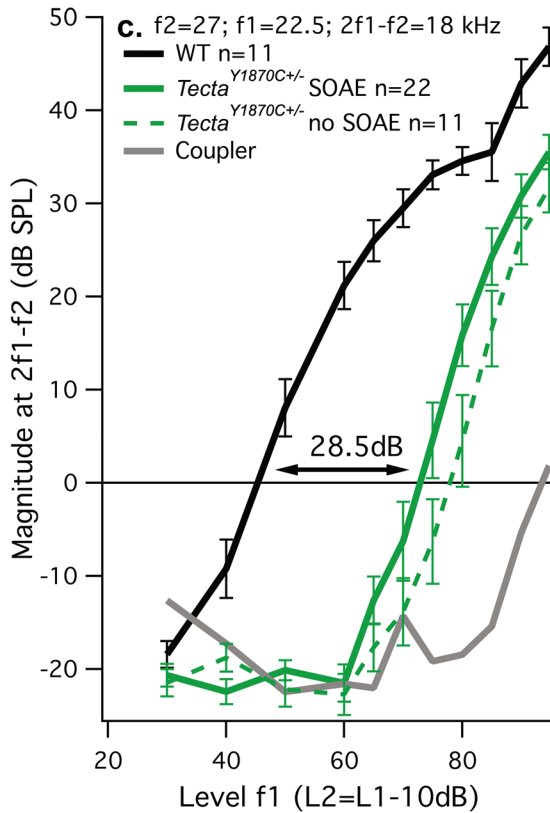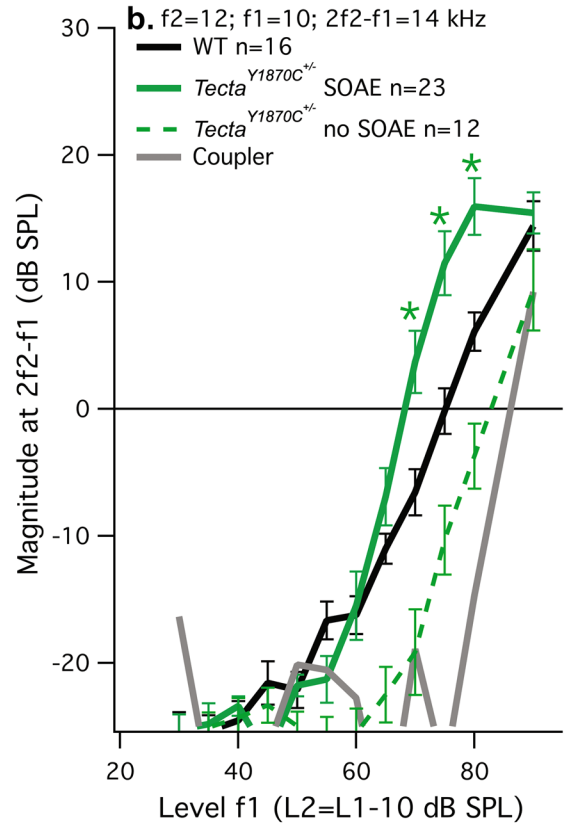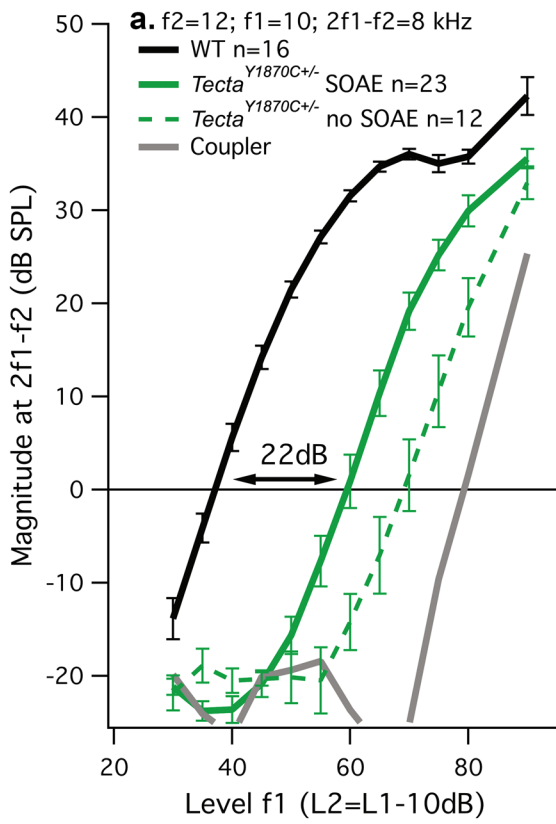
◀**Fig. 4** Input-output functions for $Tecta^{Y1870C+/-}$ mice and their controls. Growth functions are provided for 2f1-f2 (panels **a** and **c**) and for 2f2-f1 (panels **b** and **d**), and for f2 = 12 kHz (panels **a** and **b**) and for f2-27 kHz (panels **c** and **d**). The horizontal line designates DPOAE threshold, i.e., the level of f1 (L1) that generates a DPOAE of 0 dB SPL. Distortion in the sound is indicated by the coupler measurements plotted in gray. The average threshold shift between WT and heterozygotes with SOAEs is represented by the horizontal arrow in panels **a** and **c** for 2f1-f2. Data for the mutants are in green; those for controls in black. Results for mutants without SOAEs are plotted with dashed lines. Asterisks in panel **b** indicate statistical significance ($p < 0.02$, ANOVA followed by the Tukey's multiple comparisons tests). In other words, $Tecta^{Y1870C+/-}$ mice with SOAEs generate larger responses than controls at 2f2-f1 when f2 = 12 kHz

SOAEs was made for the other 14 mutants as the phenotype had not yet been discovered. Although some of the 14 $Ceacam16^{-/-}$ mice likely had SOAEs, it is not known which ones they were. In contrast, DP grams at the lower level were collected for 31 mutants with SOAEs and 22 mutants without SOAEs. At this lower stimulus level, no statistically significant differences were found between mice lacking $Ceacam16$ and their controls but only for mutants generating SOAEs (dashed lines). $Ceacam16^{-/-}$ mice lacking SOAEs (dot-dashed lines) had smaller responses at 2f1-f2 for the DP gram collected at L1 = 50 L2 = 35 dB SPL when compared to WT. The functions in Fig. 1b show 2f2-f1 plotted at f2 when L1=L2 = 70 dB SPL. To better compare WT (black) and mutant (red), the USB data are replotted in panel c at the DPOAE frequency, i.e., at 2f2-f1. Average SOAE frequency ($\pm$ SD) for $Ceacam16^{-/-}$ mice is shown along the abscissa using the horizontal arrow. The results indicate that $Ceacam16^{-/-}$ mice produced larger DPOAEs at 2f2-f1 than WT, but only in the frequency region where SOAEs were also observed. Asterisks in Fig. 1c indicate that the DPOAEs at 2f2-f1 were statistically larger in mutants (n = 19, $p < 0.02$). The correlation between SOAEs and the enhanced responses at 2f2-f1 is consistent with data collected on older $Ceacam16^{-/-}$ mice at ~ 7 months of age when SOAEs are rare [22]. In Fig. 2a, the DPOAEs at 2f1-f2 were smaller in knockouts lacking SOAEs at ~ 7 months of age. In contrast to adolescent KOs, the DPOAEs at 2f2-f1 were smaller than those in controls (Fig. 2b). In other words, older $Ceacam16^{-/-}$ without SOAEs did not produce larger magnitudes at 2f2-f1 than WT mice. By one year of age null mutants produce no emissions of any kind [22].

$Tecta^{Y1870C+/-}$ Mice

Iso-input functions at 70 dB SPL were also collected for heterozygous mice with a missense mutation in $Tecta$, $Tecta^{Y1870C}$. Results indicate that 63% of these mutants generate SOAEs when they express only one copy of the mutated gene [17]. In contrast to young mice lacking $Ceacam16$, $Tecta^{Y1870C}$ heterozygotes with SOAEs (green solid lines) had

reduced DPOAEs at 2f1-f2 (Fig. 3a). Mutants lacking SOAEs (green dashed lines) had even smaller responses. In contrast, the responses at 2f2-f1 in mutants with SOAEs (Fig. 3b, c) were comparable to WT. Data in panel c demonstrate that 2f2-f1 in mutants with SOAEs can exceed that in controls but only in the frequency region where SOAEs were recorded. The horizontal bar above the abscissa shows the average SOAE frequency $\pm$ SD (15.4 $\pm$ 7.0 kHz). Although mutants with SOAEs were not statistically different from controls, the increases at 2f2-f1 in heterozygous mice with SOAEs (green solid lines) approached statistical significance ($p = 0.11$) at f2 = 13.5 kHz and where 2f2-f1 = 15.8 kHz.

DPOAE input-output functions are plotted in Fig. 4. Panels a and b show data for f2 = 12 kHz; panels c and d for f2 = 27 kHz. For heterozygotes with SOAEs (green solid lines), the average threshold shift was 22 dB SPL for the LSB component at 2f1-f2 = 8 kHz (Fig. 4a). Mutants without SOAEs (green dashed lines) had larger threshold shifts and failed to generate SOAEs. For input-output functions collected at 2f2-f1 = 14 kHz, the USB DPOAE, the average threshold in mutants with SOAEs was statistically lower than WT (see Table 1), and the responses exceeded those in controls as level increased (Fig. 4b). For f1 levels (L1) between 70 and 80 dB SPL, responses for the USB DPOAE at 2f2-f1 were statistically larger than WT ($p < 0.02$). For mutants lacking SOAEs, the responses were smaller than WT at all levels. At f2 = 27 kHz, DPOAEs in controls exceeded those in all mutants for both 2f1-f2 = 18 kHz (Fig. 4c) and 2f2-f1 = 31.5 kHz (Fig. 4d). In $Tecta^{Y1870C+/-}$ with SOAEs, the LSB component at 2f1-f2 was shifted to the left by 28.5 dB relative to controls. In this high-frequency region, no SOAEs were observed and DPOAEs were reduced relative to controls for emissions both above and below the primaries. As observed in Fig. 3, larger reductions were recorded in $Tecta^{Y1870C+/-}$ lacking SOAEs (green dashed lines).

$Tectb^{-/-}$ Mice

As reported previously [19], mice lacking $Tectb$ showed a large reduction in 2f1-f2 at low f2 frequencies where the thickness of the TM increases. However, at high f2 frequencies, the magnitudes at 2f1-f2 were commensurate with those in controls at 70 dB SPL. It is in this high-frequency region that mice lacking $Tectb$ produced SOAEs although the incidence was only 17%. Average DPOAEs at 2f1-f2 (Fig. 5a) and 2f2-f1 (Fig. 5b) were plotted at f2 for $Tectb^{-/-}$ with SOAEs (n = 6, solid blue lines) and without SOAEs (n = 27, blue dashed lines). In general, mice lacking $Tectb$ had reduced DPOAEs at 2f1-f2 for f2 frequencies below 30 kHz. The red traces show responses from the two $Tectb^{-/-}$ mice with the largest SOAEs. In Fig. 5c, 2f2-f1 is plotted at the DPOAE frequency and the full range of SOAE frequencies is represented by the horizontal arrow along the abscissa (average
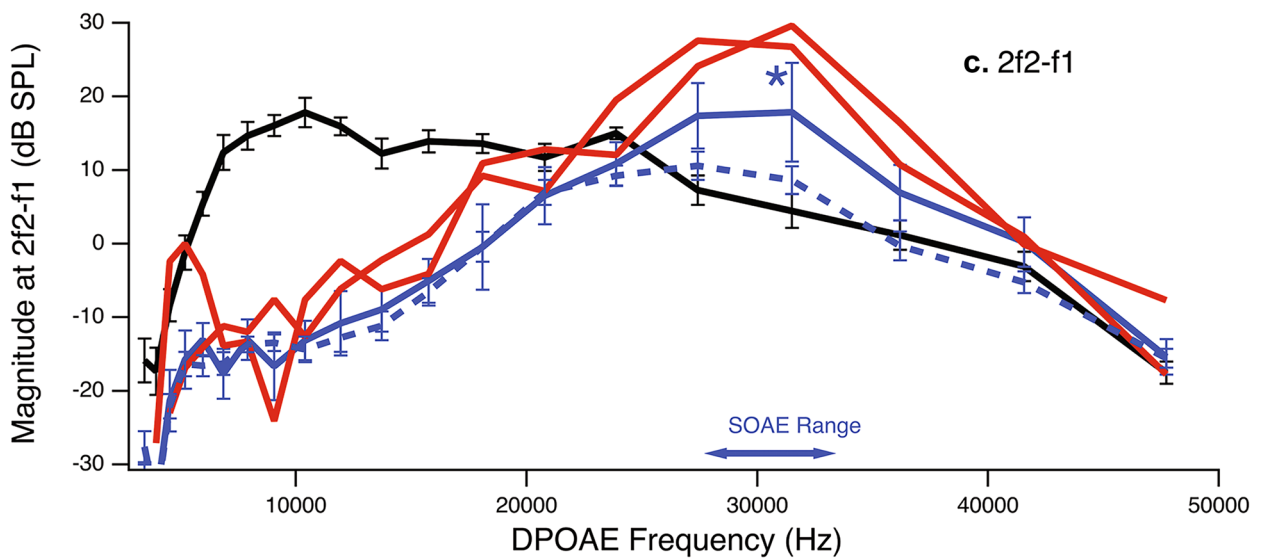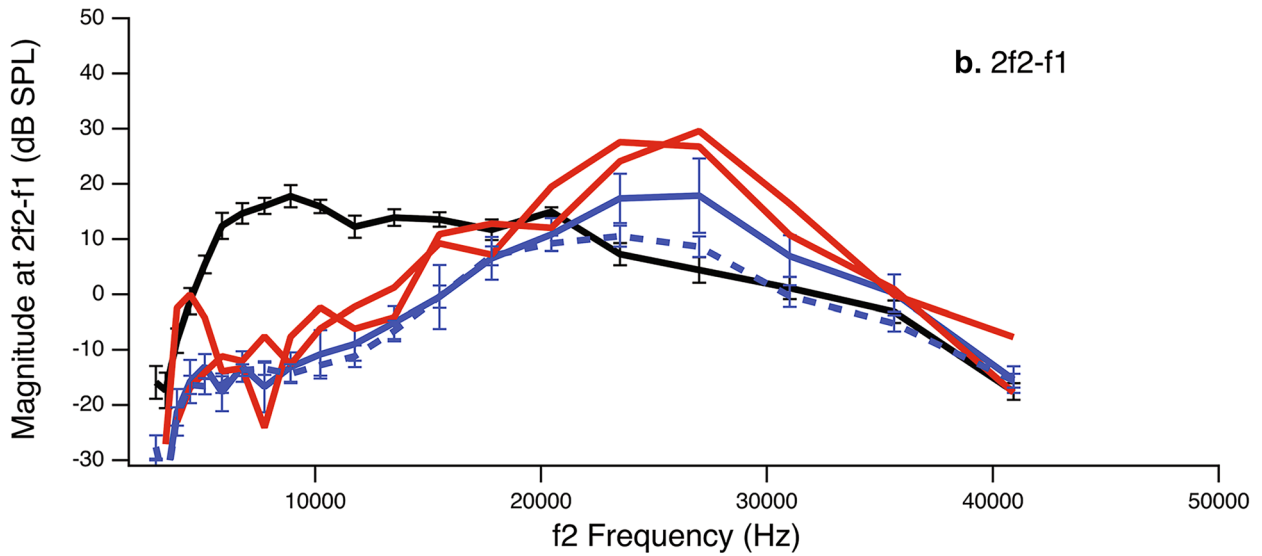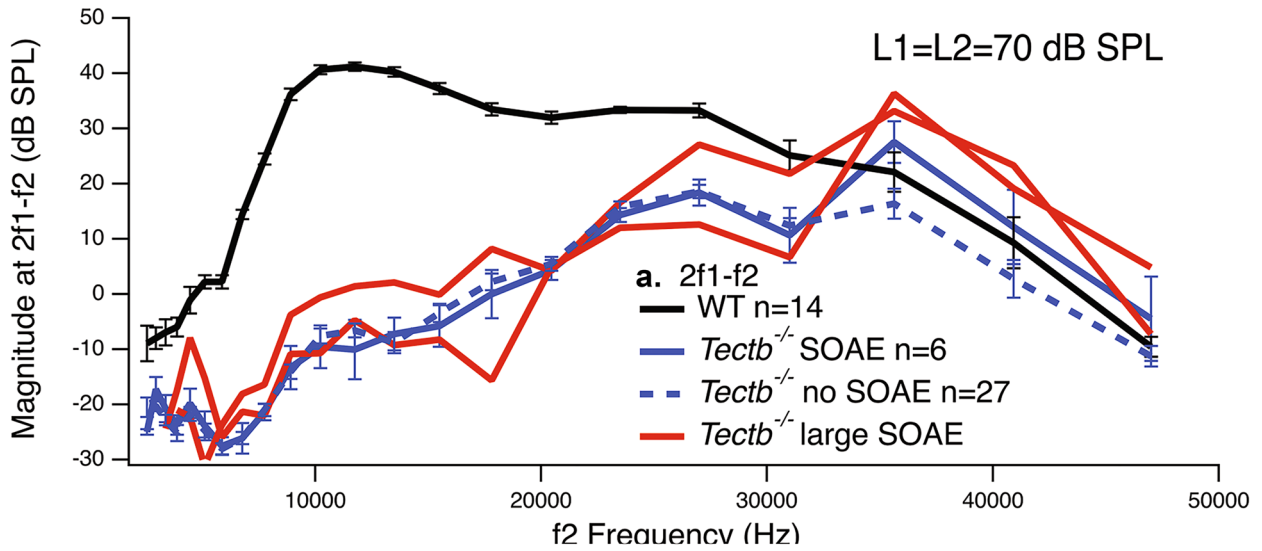
a. 2f1-f2
WT n=14
Tectb$^{-/-}$ SOAE n=6
Tectb$^{-/-}$ no SOAE n=27
Tectb$^{-/-}$ large SOAE

L1=L2=70 dB SPL

b. 2f2-f1

c. 2f2-f1

SOAE Range

◄ **Fig. 5** Iso-input functions for *Tectb*$^{-/-}$ mice and their controls. The blue solid lines show results for *Tectb*$^{-/-}$ knockouts with SOAEs (n = 6), while the blue dashed lines show magnitudes for mutants without SOAEs (n = 27). The two mice lacking *Tectb* that produced the largest SOAEs are shown in red. In contrast to previous figures, the full range of SOAE frequencies is represented along the abscissa with the horizontal arrow in panel **c**. When the USB DPOAE at 2f2-f1 is plotted at the DPOAE frequency, the responses in knockouts with SOAEs exceeded those in controls. The asterisk indicates a significant increase in the USB distortion product when 2f2-f1 = 31.5 kHz, the average SOAE frequency. The adjusted *p* value, 0.02, was obtained using ANOVA followed by Tukey's multiple comparisons tests

SOAE frequency = 31.5 kHz). In this region, 2f2-f1 can be larger in spontaneously emitting mutants, especially in *Tectb*$^{-/-}$ mice with prominent SOAEs. The asterisk indicates that *Tectb*$^{-/-}$ mice with SOAEs generate larger responses for the USB DPOAE at 2f2-f1 than do their controls when f2 = 27 kHz (*p* = 0.02).

Input-output functions are also provided in Fig. 6 for f2 = 27 kHz where 2f1-f2 = 18 kHz (panel a) and 2f2-f1 = 31.5 kHz (panel b). Even though reductions are observed in *Tectb*$^{-/-}$ at 2f1-f2, the average magnitudes of USB emissions at 2f2-f1 in mutants with SOAEs can exceed those in controls. Although not shown, there was no enhancement of 2f2-f1 in *Tectb*$^{-/-}$ when f2 = 32 kHz and 2f2-f1 = 37.3 kHz. Hence, the USB DPOAE can be larger in mutants, but only when they generate SOAEs and only when the frequency of the distortion product is similar to the frequency of the SOAE. Responses at 2f2-f1 were statistically larger in knockouts with versus without SOAEs as shown by the asterisks (*p* < 0.02). Although *Tectb*$^{-/-}$ with SOAEs were not statistically different from WT, the difference approached significance at L1 = 80 dB SPL where the adjusted *p* value was 0.07.

It is also acknowledged that mice lacking *Tectb* have frequency dependent ABR threshold shifts that are similar to those for the DPOAEs. In WT controls, the average ABR threshold (± SD) was 18.7 ± 3.4 dB at 12 kHz (n = 7), 22.3 ± 5.6 dB at 27 kHz (n = 6), and 27.9 ± 6.0 dB at 32 kHz (n = 10). In contrast, the average ABR threshold in *Tectb*$^{-/-}$ mice was 64.9 ± 7.3 dB at 12 kHz (n = 17), 39.0 ± 6.1 dB at 27 kHz (n = 17) and 41.8 ± 13.7 dB at 32 kHz (n = 13). Hence, threshold shifts for mice lacking *Tectb* and their controls were 46.2 dB at 12 kHz, 16.7 dB at 27 kHz and 13.9 dB at 32 kHz. The larger changes in sensitivity at the lower frequencies are consistent with previous measurements and with the increase in area of the TM in apical regions of the cochlea [19].

Mice Lacking Somatic Electromotility

DPOAE input-output functions at f2 = 12 kHz were acquired in mice lacking prestin and are plotted in Fig. 7 as a function of the level of f1 (L1) where the level of f2 (L2)

was 10 dB lower than that of f1. Loss of prestin reduces 2f1-f2 (magenta solid line) but the responses at 2f2-f1 (magenta dashed line) are WT-like (black). Similar results were obtained for knockin mice expressing a nonfunctional prestin but are not plotted for clarity. These results, however, are included in Table 1 (see *Slc26a5*$^{V499G/Y499H}$). Prestin KO (*Slc26a5*$^{-/-}$) mice show a threshold shift of 32 dB SPL at 2f1-f2 (LSB KO-WT), but the difference is less than 5 dB SPL at 2f2-f1 (dashed lines). Data from WT controls (black) indicate that the USB component at 2f2-f1 is amplified much less that 2f1-f2. It is also apparent that the input-output function for 2f1-f2 in the controls shows cochlear compression, which is not obvious for 2f2-f1 or for the results obtained in mice lacking somatic electromotility. This observation is consistent with passive nonlinear processes, i.e., lack of amplification. In WT mice, the average threshold at 2f2-f1 is 37 dB higher than for 2f1-f2 (WT USB-LSB), i.e., 2f2-f1 is much smaller than 2f1-f2 in controls. Hence, the lack of prestin has a minimal effect on the USB component at 2f2-f1. Independent of genotype, all responses tend to converge at high stimulus levels. Previous publications on prestin mouse models lacking somatic electromotility have also documented large threshold shifts for auditory brainstem responses and compound action potentials [5–7]. The reductions in sensitivity are consistent with those for the DPOAEs.

Thresholds for USB and LSB DPOAEs

Average DPOAE threshold shifts for all mutants and their controls were obtained using input-output functions and when the level of f1 exceeded the level of f2 by 10 dB SPL. These results are provided in Table 1 for f2 = 12 kHz and f2 = 27 kHz. In WT mice, thresholds at 2f2-f1 are 30–40 dB higher than at 2f1-f2. This difference in threshold for USB versus LSB emissions is similar to the threshold shift for 2f1-f2 in *Slc26a5*$^{-/-}$ (prestin KO) mice at f2 = 12 kHz (32 dB SPL). Data are also provided for DPOAEs acquired in mice expressing a mutant form of prestin that is nonfunctional in vivo. This latter mouse model was required because OHCs lacking prestin are short and flaccid, which by itself could result in loss of cochlear amplification. Hence, 499 prestin knockin (*Slc26a5*$^{V499G/Y499H}$) mice were developed. In these mutants, where OHCs are normal in length and stiffness, large threshold shifts were recorded at 2f1-f2 similar to mice lacking prestin [5, 23]. Because the input-output functions for 499 prestin KIs collected at f2 = 12 kHz were virtually identical to those collected in prestin KOs, they were not included in Fig. 7. Data tabulated in Table 1 indicate loss of gain in mice lacking electromotility, or partial loss of gain in TM mutants, increases thresholds for 2f1-f2, while thresholds for 2f2-f1 remain relatively stable and wildtype-like. Even though thresholds in TM mutants at
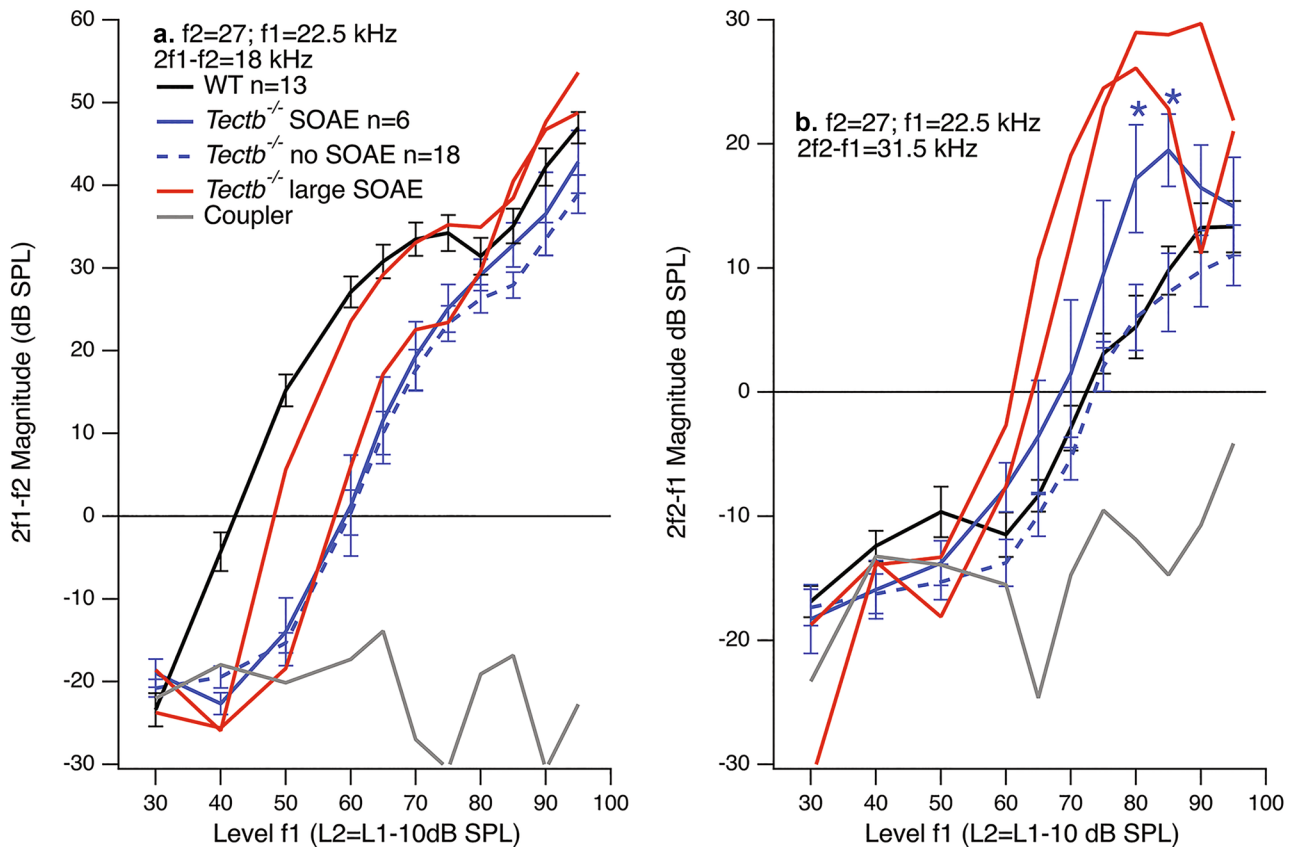
Fig. 6 Input-output functions at f2 = 27 kHz for mice lacking *Tectb* and their controls. Panel **a** shows magnitude for 2f1-f2 = 18 kHz, while panel **b** shows 2f2-f1 = 31.5 kHz. Data are provided for the WT controls (black), for mutants with SOAEs (blue solid lines, n = 6), for mutants without SOAEs (blue dashed lines, n = 18) and for the two mutants with the largest SOAEs (red traces). Coupler distortion is plotted in gray. Asterisks indicate that *Tectb*−/− with SOAEs had larger DPOAEs at 2f2-f1 than *Tectb*−/− without SOAEs (*p* < 0.02, ANOVA followed by Tukey's multiple comparisons tests)

2f1-f2 are better than in the prestin mutants, those at 2f2-f1 are similar to mice lacking somatic electromotility and to the controls. It is also emphasized that WT thresholds at 27 kHz are higher than at 12 kHz by ~8 dB. Hence, the change due to mutation is ~30 dB for 2f2-f1 and 40 dB at 2f1-f2. However, if one compensates for the 8 dB, then 2f2-f1 is shifted ~40 dB at both f2 frequencies. Although 2f2-f1 was larger in *Tectb*−/− and *Tecta*Y1870C+/− mice (positive numbers in Table 1), the increase was statistically greater than in controls for only the *Tecta*Y1870C heterozygotes (adjusted *p* value was 0.006).

Results provided in Table 1 are also represented as bar graphs in Fig. 8 using the same color code as in previous figures. Panel a provides average DPOAE threshold shifts re: WT for 2f1-f2 when f2 = 12 kHz. In the lower panel b, data are plotted for 2f2-f1. Results on the right show threshold shifts for f2 = 27 kHz with data for 2f1-f2 in the top panel c and for 2f2-f1 in the bottom panel d. Input-output functions were only collected at f2 = 12 kHz in the prestin mutants. *Ceacam16* mutants (n = 19) are near normal. In contrast,

larger threshold shifts were observed in the other mutants at 2f1-f2 (top panels). By comparison, threshold shifts for the USB at 2f2-f1 were relatively small. In fact, the threshold for 2f2-f1 when f2 = 12 kHz (panel c) was statistically lower in *Tecta*Y1870C heterozygotes than in controls.

Discussion

In WT mice, the USB DPOAE at 2f2-f1 is much smaller than the LSB DPOAE at 2f1-f2. Although 2f2-f1 is also smaller in humans [24, 25], the relative differences are larger in mice. These distinctions between mice and humans are not unexpected given the differences in their audiograms and the fact that mechanical filtering and cochlear roughness are likely species dependent. Data from TM mutants also indicate that partial loss of gain reduces 2f1-f2, but 2f2-f1 remains WT-like. In mutants with SOAEs, the USB DPOAEs can be even larger than in controls. Enhanced responses at 2f2-f1 in TM mutants with SOAEs suggest

Fig. 7 Input-output functions at f2 = 12 kHz for mice lacking prestin (*Slc26a5*$^{-/-}$, magenta) and their controls (black). The data for 2f1-f2 are plotted with solid lines, those for 2f2-f1 with dashed lines. Coupler values are in gray. The horizontal magenta arrow indicates that loss of prestin reduces 2f1-f2 by 32 dB SPL (LSB KO-WT). The horizontal black arrow shows a 37 dB difference in threshold between 2f1-f2 and 2f2-f1 (USB-LSB) in WT controls
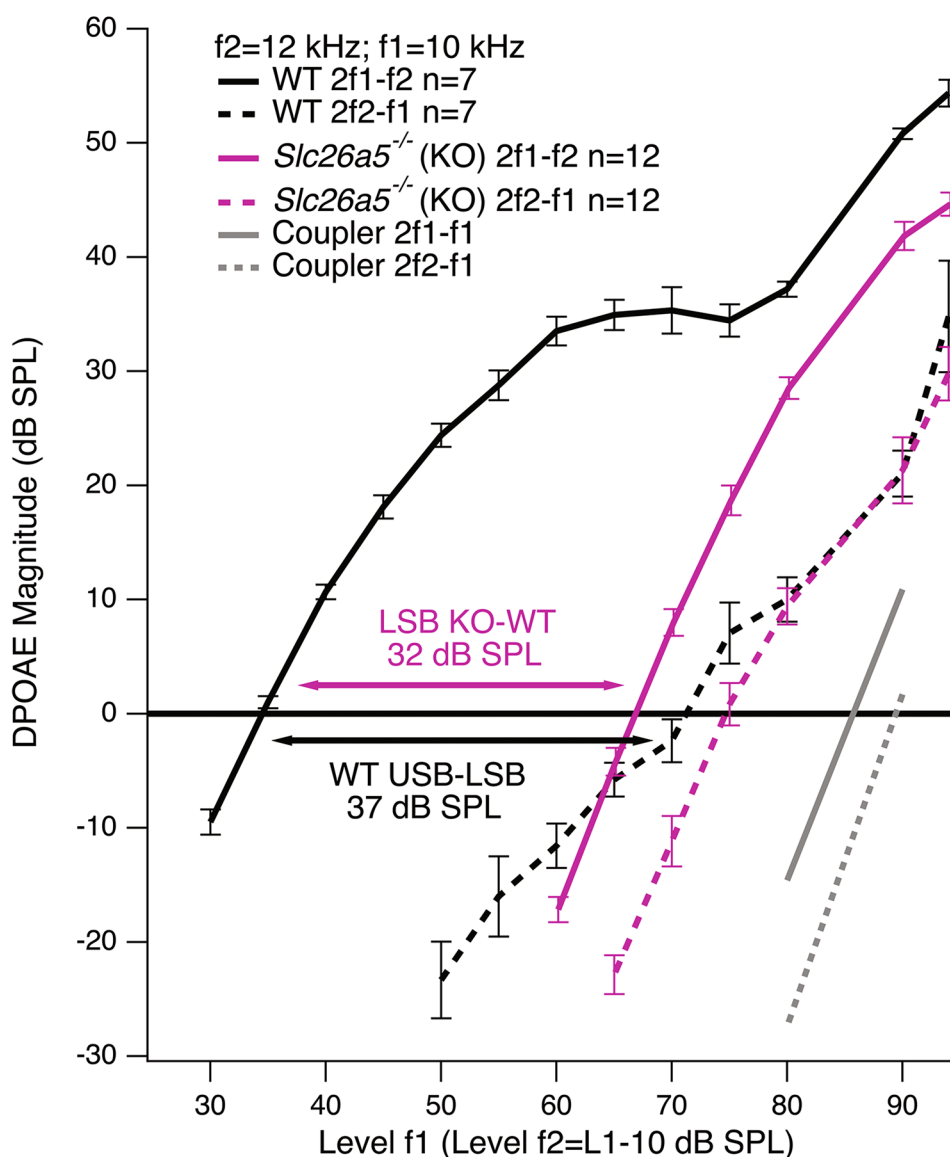
the possibility that rabbits with larger 2f2-f1 after noise exposure [3] may have developed SOAEs, as previously reported for chinchillas [26]. In mice lacking prestin, 2f1-f2 is reduced by up to 50 dB [12], but 2f2-f1 is similar to controls [27]. Hence, loss of somatic electromotility in prestin mutants produces minimal changes in the USB DPOAE that are not statistically different from controls.

It should also be understood that emissions can only be generated if cochlear amplification is operational to some degree [28]. The fact that mice lacking somatic electromotility produce DPOAEs indicates that mechanical nonlinearities associated with the stereocilia are the likely source of this distortion [12, 13] and that the mechanoelectrical transducer channels are operational, as verified experimentally in prestin mutants [5, 29]. *Tecta*^{Y1870C} heterozygotes [18] and *Tectb* knockouts [19] also produce a normal CM, which is

a gross reflection of hair cell receptor currents. Although the CM and/or mechanoelectrical transducer currents have not been measured for mice lacking *Ceacam16,* these animals have WT-like DPOAEs and ABRs when young, which implies that transducer function is normal as well. The fact that generation of cubic intermodulation distortion relates to nonlinear hair-bundle mechanics is consistent with a distortion component analysis of the OHC's motility-related gating charge showing that prestin's motor action is weakly nonlinear and quadratic in nature [30, 31]. Although electromotility can make cochlear distortion products and emissions larger, it is unlikely to be their source. The latter is dominated by a nonlinear mechanoelectrical transduction process [12, 13]. Hence, the LSB DPOAE at 2f1-f2 is associated with a nonlinear transducer current and receives enhancement due to prestin's motor activity. The fact that

the USB DPOAE at 2f2-f1 is similar in mice lacking prestin and their controls suggests that this component is associated with nonlinear hair bundle mechanics but is not amplified by somatic electromotility.

Because IMD products with frequencies greater than the primaries do not propagate basally [32–34], Brown and Kemp [35] suggested that 2f2-f1 was generated basal to its DP place, allowing it to then propagate apically and to be amplified. In fact, Kemp [36] referred to wave-fixed versus place-fixed mechanisms of emission generation. Wave-fixed sources were those in the region of overlap between the two stimulating primaries, while place-fixed sources were those located at the best frequency (BF) of the distortion product. In this latter case, IMD components were generated in the region of overlap and then propagated apically to their BF or DP place along the cochlear partition. Somewhat later, Shera and Guinan [37] used the terms distortion (wave-fixed) versus linear-reflection (place-fixed) emissions, respectively. Because of the relatively high levels of stimulation required to record 2f2-f1 from the mouse ear canal, these distinctions are complicated. At 70 dB SPL, the excitation patterns for the primaries are broad, with peaks closer to the base than the BF locations for f1 and f2. Given that the distortion region is likely to include the reflection site at the 2f2-f1 place, one cannot assume that 2f2-f1 is necessarily "reflected" from the DP place [38].

The influence of stimulus parameters has been investigated in modeling studies of 2f2-f1 [39, 40]. At high levels, and with a frequency ratio of 1.2, the canal pressure is dominated by IMD generated in the region of overlap between the two primaries, and primarily by OHC generators with BFs between f2 and the 2f2-f1 frequency. This region was also proposed as the source for 2f2-f1 in rabbits [41], where reflection components could not be measured by placing a suppressor or interference tone near the DP place. Targeted inducement of temporary threshold shifts also demonstrated that 2f2-f1 was generated basal to f2 [42].

Data in Table 1 indicate that thresholds for the DPOAE at 2f1-f2 are ~ 35 dB SPL in controls. In contrast, the thresholds at 2f2-f1 are 70–75 dB SPL. When using a relatively large frequency ratio, such as f2/f1 = 1.2, the LSB DPOAE at 2f1-f2 appears to be associated with distortion sources in the region of overlap between the primaries in both human subjects [38, 43] and laboratory animals [42, 44, 45]. Cochlear

Table 1 DPOAE thresholds for all mutants and their controls (*p < 0.02)

| Mouse Model	f2 = 12 kHz 2f1-f2	f2 = 12 kHz 2f2-f1	f2 = 27 kHz 2f1-f2	f2 = 27 kHz 2f2-f1
Ceacam16 **WT**	37.0 ± 2.9 n = 19	78.2 ± 5.8 n = 19	45.0 ± 5.1 n = 11	75.9 ± 7.2 n = 11
Ceacam16$^{-/-}$	39.5 ± 4.3 n = 19	77.6 ± 6.4 n = 19	47.3 ± 5.6 n = 15	77.2 ± 10.1 n = 15
WT-*Ceacam16*$^{-/-}$	-2.5	+0.6	-2.3	-1.3
WT (2f1-f2)-(2f2-f1)		-41.2		-30.9
Tectb **WT**	34.3 ± 2.2 n = 13	73.6 ± 5.0 n = 13	42.2 ± 4.5 n = 13	73.8 ± 6.1 n = 13
Tectb$^{-/-}$ **SOAE**	76.7 ± 3.7 n = 6*	85.4 ± 5.5 n = 6*	59.5 ± 7.0 n = 6*	69.4 ± 8.0 n = 6
Tectb$^{-/-}$ **no SOAE**	76.2 ± 2.7 n = 18*	83.9 ± 5.1 n = 18*	59.1 ± 4.9 n = 18*	76.7 ± 8.4 n = 18
WT-*Tectb*$^{-/-}$ **SOAE**	-42.4	-11.8	-17.3	+4.4
WT (2f1-f2)-(2f2-f1)		-39.3		-31.6
Tecta^{Y1870C} **WT**	37.5 ± 3.3 n = 16	75.3 ± 6.6 n = 16	45.4 ± 6.8 n = 11	74.4 ± 7.0 n = 11
Tecta$^{Y1870C+/-}$ **SOAE**	59.5 ± 6.4 n = 23*	68.3 ± 7.0 n = 23*	73.9 ± 8.1 n = 22*	81.9 ± 6.9 n = 22*
Tecta$^{Y1870C+/-}$ **no SOAE**	69.3 ± 7.7 n = 12*	81.5 ± 5.8 n = 12	78.4 ± 6.6 n = 11*	85.9 ± 6.1 n = 11*
WT-*Tecta*$^{Y1870C+/-}$ **SOAE**	-22.0	+7.0*	-28.5	-7.5
WT (2f1-f2)-(2f2-f1)		-37.8		-29.0
Slc26a5 **WT**	34.5 ± 0.8 n = 7	72.0 ± 4.3 n = 7		
Slc26a5$^{-/-}$	66.8 ± 1.6 n = 12*	74.8 ± 3.3 n = 12		
Slc26a5$^{V499G/Y501H}$	64.8 ± 2.1 n = 9*	75.9 ± 3.1 n = 9		
WT- *Slc26a5*$^{-/-}$	-32.3	-2.8		
WT- *Slc26a5*$^{V499G/Y501H}$	-30.3	-3.9		
WT (2f1-f2)-(2f2-f1)		-37.5		

This table summarizes the average thresholds (± SD) obtained in TM mutants lacking *Ceacam16,* lacking *Tectb*, as well as mice heterozygous for a missense mutation in *Tecta* (*Tecta*$^{Y1870C+/-}$). Results are also provided for mice lacking prestin (*Slc26a5*$^{-/-}$) or expressing non-functional 499 prestin (*Slc26a5*$^{V499G/Y499H}$). Except for the prestin mutants, thresholds are tabulated for f2 = 12 kHz and f2 = 27 kHz. Positive numbers (red) indicate that the mutant is better than WT. It is also emphasized that the group of mice lacking *Ceacam16* was composed of animals with and without SOAEs. Asterisks indicate statistical significance. The *p* values, independent of whether they were obtained using the Student's t-test (*Ceacam16* only) or ANOVA followed by Tukey's multiple comparisons tests, were less than 0.02 when mutants were compared with WT controls

The asterisks indicate statistical significance

models [40, 46] also indicate that 2f1-f2 originates from distortion sources near f2, while 2f2-f1 is associated with more basal generators between f2 and the DP place. These predictions are consistent with work indicating that individual cubic distortion components may relate to different locations along the cochlear partition [42]. The possibility that distortion, due to the overlapping excitation patterns of the two primaries, could dominate both USB and LSB emissions in mice may relate to the knowledge that waves associated with reflection sites are especially vulnerable to rapid extinction [40]. In addition, stimulus levels greater than ~ 45 dB SPL are predicted to increase contributions from nonlinear sources to the DPOAE at 2f2-f1 [47].

Data in TM mutants with SOAEs also indicate that 2f2-f1 can be larger than in controls when the frequency of the distortion product coincides with the frequency region generating SOAEs. It is notable, however, that larger magnitudes at 2f1-f2 were not observed. This observation is consistent with evidence showing that the ear canal pressure primarily reflects outputs from OHCs located in the region of overlap between the two stimulating primaries, especially when presented at moderate levels and for f2/f1 = 1.2 as in this report [38, 48–50]. When f1 = 29.7 kHz and f2 = 35.6 kHz, 2f1-f2 = 23.8 kHz, which is similar to the average SOAE frequency in mice lacking *Ceacam16*. For these stimulus conditions, increased magnitudes were not recorded for the

Fig. 8 Threshold shifts for upper and lower side band DPOAEs are plotted as bar graphs using data in Table 1. For each mutant, thresholds were normalized relative to WT to highlight the differences between mouse models. Each panel is devoted to a single f2 frequency and to either the LSB or the USB distortion product. Panels **a** and **c** show results for f2 = 12 kHz; panels **b** and **d** for f2 = 27 kHz. Relative thresholds for 2f1-f2 (LSB) are plotted in panels **a** and **b**; for 2f2-f1 (USB) in panels **c** and **d**. Asterisks indicate statistical significance (*p* < 0.02, ANOVA followed by Tukey's multiple comparisons tests). For the *Tecta* and *Tectb* mutants, the threshold shifts are between mutants with SOAEs and their controls. For mice lacking *Ceacam16*, the mutants included mice with and without SOAEs
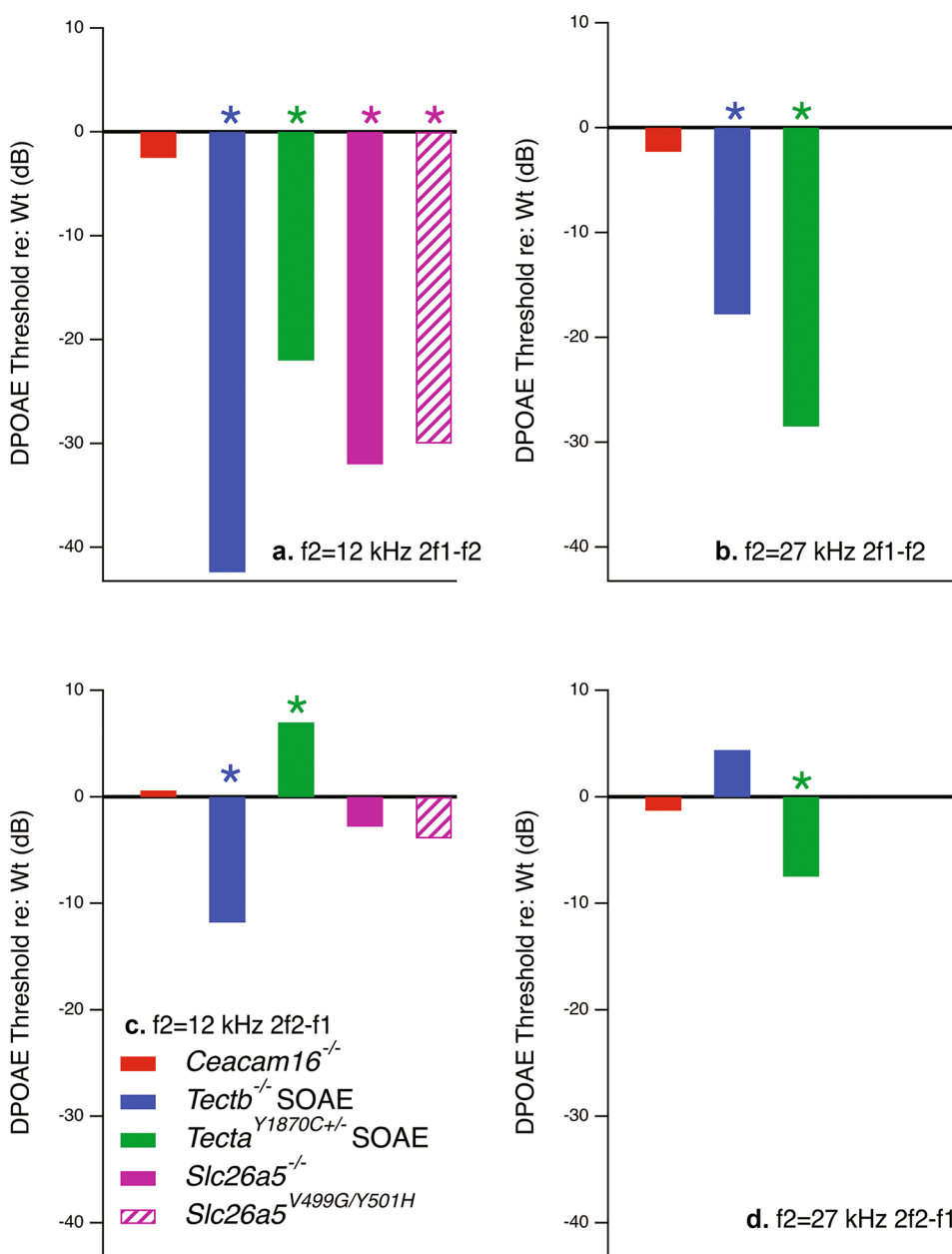
LSB DPOAE at 2f1-f2, i.e., there were no statistically significant differences in the average DP grams of controls versus mice lacking *Ceacam16* at either L1 = L2 = 70 dB SPL or at L1 = 50 L2 = 35 dB SPL (Fig. 1a). This observation implies that the emission at 2f1-f2 was not dominated by contributions from the more apical DP place. The absence of changes in 2f1-f2 also suggests that SOAEs do not increase IMD by increasing stimulation by the primaries at the generation sites. If this were the case, all components should increase not just the USB component at 2f2-f1. Although enhancements at 2f2-f1 in mutants with SOAEs might relate to an increase in the reflection mechanism, this possibility was not specifically tested. However, if the reflection mechanism did increase in TM mutants, then 2f1-f2 should also increase for high-frequency primary pairs generating a 2f1-f2 that travels apically to the DP place and where the SOAEs are being generated. Again this was not observed in mice lacking *Ceacam16.*

The low magnitudes of USB DPOAEs observed in normal mice may relate to several complicating factors. Given that thresholds for 2f2-f1 are at least 70 dB SPL in WT controls, contributions from OHCs with BFs greater than f2 are to be expected given the basal extension of the excitation patterns for the two high-level primaries [51–53]. Hence, the BF locations of f1 and f2 are apical to the BFs of OHCs dominating 2f2-f1. The relatively small responses at 2f2-f1 may, therefore, relate to a reduction in cochlear gain due to the high stimulus levels required for their observation [54], and to the more linear responses produced by OHCs activated by primaries below their individual BFs [24].

Measurements in the ear canal are further complicated by phase cancellation of responses produced by individual hair cell generators located at different positions along the cochlear partition [55]. Work in laboratory animals [44] indicates that phase cancellation reduces 2f1-f2 primarily for narrow f2/f1. In contrast, rapid phase variations were encountered with all frequency ratios for 2f2-f1. This latter observation implies that phase cancellation may impact 2f2-f1 to a greater degree than for 2f1-f2. In addition, distortion products observed in mechanical vibrations within the organ of Corti may differ from those measured in the mouse ear canal, i.e., the latter observations do not necessarily provide an accurate representation of intracochlear nonlinear processes [56]. Finally, differences between DPOAEs above and below the eliciting primaries could also relate to the upward spread of masking [57, 58]. As masker level increases, threshold shifts are greater for signals above the masker frequency. Hence, the USB DPOAE could be suppressed by the primaries with the result that 2f2-f1 is smaller than 2f1-f2. Because 2f1-f2 is below f1 in frequency, it is less vulnerable to masking from the primaries. All of these factors probably contribute to the higher thresholds observed for the USB distortion component in WT control animals.

Taken together, the results in mice indicate that 2f2-f1 is not a sensitive indicator of changes in sensitivity. Mice with partial loss of gain, or with loss of somatic electromotility, both generate USB IMD components that are WT-like. Hence, the DPOAE at 2f2-f1 is not useful in the diagnosis of hearing loss. Because of the relatively high levels required to observe 2f2-f1, this emission is impacted by several complicating factors. These include phase cancellation, upward spread of masking and the likelihood that this component is dominated by OHCs responding more linearly of the tails of their tuning curves.

Data Availability Data in this manuscript can be made available to interested parties by contacting the author.

Declarations

Conflict of Interest The author declares that there are no conflicts of interest.

References

1. Kim DO (1980) Cochlear mechanics: implications of electrophysiological and acoustical observations. Hear Res 2(3–4):297–317. PubMed PMID: 7410234

2. Siegel J (2008) Otoacoustic emissions. In: Basbaum AI, Kaneko A, Shepherd G, Westheimer G (eds) The Senses: A Comprehensive Reference. Academic Press, San Diego, pp 237–262

3. Lonsbury-Martin BL, Martin GK (2008) Otoacoustic emissions: Basic studies in mammalian models. In: Manley G, Fay R, Popper A (eds) Active Processes and Otoacoustic Emissions. Springer, New York NY, pp 261–303

4. Zheng J, Shen W, He DZ, Long KB, Madison LD, Dallos P (2000) Prestin is the motor protein of cochlear outer hair cells. Nature 405(6783):149–155. PubMed PMID: 10821263

5. Dallos P, Wu X, Cheatham MA, Gao J, Zheng J, Anderson CT, Jia S, Wang X, W.H.Y. C, Sengupta S, He DZZ, Zuo J (2008) Prestin-based outer hair cell motility is necessary for mammalian cochlear amplification. Neuron 58:1–7

6. Liberman MC, Gao J, He DZ, Wu X, Jia S, Zuo J (2022) Prestin is required for electromotility of the outer hair cell and for the cochlear amplifier. Nature 419(6904):300–304. Epub 2002/09/20. https://doi.org/10.1038/nature01059. PubMed PMID: 12239568

7. Cheatham MA, Huynh KH, Gao J, Zuo J, Dallos P (2004) Cochlear function in Prestin knockout mice. J Physiol 560(Pt 3):821–830. PubMed PMID: 15319415

8. Dallos P, Wang CY (1974) Bioelectric correlates of kanamycin intoxication. Audiology 13(4):277–289. PubMed PMID: 4606272

9. Ryan A, Dallos P (1975) Effect of absence of cochlear outer hair cells on behavioural auditory threshold. Nature 253(5486):44–46. PubMed PMID: 1110747

10. Brown AM, McDowell B, Forge A (1989) Acoustic distortion products can be used to monitor the effects of chronic gentamicin treatment. Hear Res 42:143–156

11. Legan PK, Lukashkina VA, Goodyear RJ, Kossi M, Russell IJ, Richardson GP (2000) A targeted deletion in alpha-tectorin reveals that the tectorial membrane is required for the gain and timing of cochlear feedback. Neuron 28(1):273–285. PubMed PMID: 11087000

12. Liberman MC, Zuo J, Guinan JJ Jr (2004) Otoacoustic emissions without somatic motility: can stereocilia mechanics drive the mammalian cochlea? J Acoust Soc Am 116(3):1649–1655. PubMed PMID: 15478431

13. Jaramillo F, Markin VS, Hudspeth AJ (1993) Auditory illusions and the single hair cell. Nature 364(6437):527–529. PubMed PMID: 8336792

14. Cheatham MA (2021) Spontaneous otoacoustic emissions are biomakers for mice with tectorial membrane defects. Hear Res 409:108314

15. Richardson GP, Lukashkin AN, Russell IJ (2008) The tectorial membrane: one slice of a complex cochlear sandwich. Curr Opin Otolaryngo 16(5):458–464. https://doi.org/10.1097/MOO.0b013e32830e20c4.PubMedPMID:WOS:000262716300011

16. Cheatham MA, Goodyear RJ, Homma K, Legan PK, Korchagina J, Naskar S, Siegel JH, Dallos P, Zheng J, Richardson GP (2014) Loss of the tectorial membrane protein CEACAM16 enhances spontaneous, stimulus-frequency, and transiently evoked otoacoustic emissions. J Neurosci 34(31):10325–10338. https://doi.org/10.1523/JNEUROSCI.1256-14.2014. PubMedPMID: 25080593; PMCID: PMC4115139

17. Cheatham MA, Zhou Y, Goodyear RJ, Dallos P, Richardson GP (2018) Spontaneous Otoacoustic Emissions in Tecta(Y1870C/+) Mice Reflect Changes in Cochlear Amplification and How It Is Controlled by the Tectorial Membrane. eNeuro 5(6):314–318. Epub 2019/01/11. https://doi.org/10.1523/ENEURO.0314-18.2018. PubMed PMID: 30627650; PMCID: PMC6325554

18. Legan PK, Lukashkina VA, Goodyear RJ, Lukashkin AN, Verhoeven K, Van Camp G, Russell IJ, Richardson GP (2005) A deafness mutation isolates a second role for the tectorial membrane in hearing. Nat Neurosci 8(8):1035–1042. https://doi.org/10.1038/nn1496. PubMed PMID: 15995703

19. Russell IJ, Legan PK, Lukashkina VA, Lukashkin AN, Goodyear RJ, Richardson GP (2007) Sharpened cochlear tuning in a mouse with a genetically modified tectorial membrane. Nat Neurosci 10(2):215–223. Epub 2007/01/16. https://doi.org/10.1038/nn1828. PubMed PMID: 17220887; PMCID: PMC3388746

20. Neely SR, Stevenson R (1992) Tech Memo No. 1. Omaha NE: Boys Town National Research Hospital

21. Neely S, Liu Z (1994) EMAV: otoacoustic emission averager. Boys Town National Research Hospital, Omaha NE

22. Goodyear RJ, Cheatham MA, Naskar S, Zhou Y, Osgood RT, Zheng J, Richardson GP (2019) Accelerated age-related degradtion of the tectorial membrane in the Ceacam16 βgal/βgal null mutant mouse, a model for late-onset human hereditary deafenss DFNB113. Front Mol Neurosci 12:147

23. Cheatham MA, Edge RM, Homma K, Leserman EL, Dallos P, Zheng J (2015) Prestin-dependence of outer hair cell survival and partial rescue of outer hair cell loss in Prestin V499G/Y501H knockin mice. PLoS ONE e0145428

24. Wilson H, Lutman M (2006) Mechanisms of generation of the 2f2-f1 distortion product otoacoustic emission in humans. J Acoust Soc Am 120

25. Botti T, Sisto R, Sanjust F, Moleti A, D'Amato L (2016) Distortion product otoacoustic emission generation mechanisms and their dependence on stimulus level and primary frequency ratio. J Acoustic Soc Am 139(2):658–673. PubMed PMID: Medline: 26936550

26. Zurek P, Clarke W (1981) Narrow-band acoustic signals emitted by chinchilla ears after noise exposure. J Acoust Soc Am 70:446–480

27. Cheatham MA, Naik K, Siegel JH, Dallos P (2011) Intermodulation DPOAEs in mice below and above the eliciting primaries. Abs Assoc Res Otolaryngol 33

28. Kemp D (2002) Otoacoustic emissions, their origin in cochlear function, and use. Br Med Bull 63:223–241

29. Jia S, He DZZ (2005) Motility-associated hair-bundle motion in mammalian outer hair cells. Nat Neurosci 8:1028–1034

30. Takahashi S, Santos-Sacchi J (1999) Distortion component analysis of outer hair cell motility-related gating charge. J Membr Biol 169(3):199–207. PubMed PMID: 10354466

31. Santos-Sacchi J (1993) Harmonics of outer hair cell motility. Biophys J 65(5):2217–2227. PubMed PMID: 8298045

32. Kim DO, Molnar CE, Matthews JW (1980) Cochlear mechanics: nonlinear behavior in two-tone responses as reflected in cochlear-nerve-fiber responses and in ear-canal sound pressure. J Acoust Soc Am 67(5):1704–1721. PubMed PMID: 7372925

33. Hall JL (1980) Cochlear models: Evidence in suppression of mechanical nonlinearities and a second filter (A review). Hear Res 2:455–464

34. Ren T (2004) Reverse propagation of sound in the gerbil cochlea. Nat Neurosci 7:333–334

35. Brown A, Kemp D (1985) Intermodulation distortion in the cochlea: could basal vibration be the major cause of round window CM distortion? Hear Res 19:191–198

36. Kemp D (1986) Otoacoustic emissions, travelling waves and cochlear mechanisms. Hear Res 22:95–104

37. Shera CA, Guinan JJ Jr (1999) Evoked otoacoustic emissions arise by two fundamentally different mechanisms: a taxonomy for mammalian OAEs. J Acoust Soc Am 105(2 Pt 1):782–798. PubMed PMID: 9972564

38. Knight RD, Kemp DT (2000) Indications of different distortion product otoacoustic emission mechaisms from a detailed f1, f2 area study. J Acoust Soc Am 107:457–473

39. Dong W, Olson E (2008) Supporting evidence for reverse cochlear traveling waves. J Acoust Soc Am 123:222–240

40. Wen H, Bowling T, Meaud J (2018) Investigation of the 2f1-f2 and 2f2-f1 distortion product otoacoustic emissions using a computational model of the gerbil ear. Hear Res 365:127–140

41. Martin GK, Stagner B, Lonsbury-Martin B (2010) Evidence for basal distortion-product otoacoustic emission compnents. J Acoust Soc Am 127:2955–2972

42. Martin GK, Lonsbury-Martin BL, Probst R, Scheinin S, Coats A (1987) Acoustic distortion products in rabbit ear canal. II Sites of origin revealed by suppression contours and pure-tone exposures. Hear Res 28

43. Knight RD, Kemp DT (2001) Wave and place fixed DPOAE maps of the human ear. J Acoust Soc Am 109:1513–1525

44. Martin G, Stagner B, Dong W, Lonsbury-Martin B (2016) Comparing distortion product otoacoustic emissions to intracochlear distortion products inferred from a noninvasive assay. J Assoc Res Otolaryngol 17:271–287

45. Withnell RH, Shaffer LA, Talmadge CL (2003) Generation of DPOAEs in the guinea pig. Hear Res 178(1–2):106–117. Epub 2003/04/10. https://doi.org/10.1016/s0378-5955(03)00064-9. PubMed PMID: 12684183

46. Dong W, Olson ES (2010) Local cochlear damage reduces local nonlinerity and decreases generator-type cochlear emissions while increasing reflector-type emissions. J Acoust Soc Am 1422–1431

47. Talmadge CL, Tubis A, Long GR, Tong C (2000) Modeling the combined effects of basilar membrane nonlinearity and roughness on stimulus frequency otoacoustic emission fine structure. J Acoust Soc Am 108(6):2911–2932. Epub 2001/01/06. https://doi.org/10.1121/1.1321012. PubMed PMID: 11144584

48. Dhar S, Long GR, Talmadge CL, Tubis A (2005) The effect of stimulus-frequency ratio on distortion product otoacoustic emission components. J Acoust Soc Am 117:3766–3776

49. Bowling T, Wen H, Meenderrnk SWF, Dong W, Meaud J (2021) Intracochlear distortion products are broadly generated by outer hair cells but their contributions to otoacoustic emissions are spatially restricted. Sci Rep 11:13651

50. Durante AS, Akhtar US, Dhar S (2022) Distortion product otoacoustic emission component behavior as a function of primary frequency ratio and primary levels. Ear Hear 43:1824–1835

51. Siegel JH, Cerka AJ, Recio-Spinoso A, van Dijk P, Ruggero MA (2005) Delays of stimulus-frequency otoacoustic emissions and cochlear vibrations contradict the theory of cohlerent refelction filtering. J Acoust Soc Am 118:2434–2443

52. Charaziak KK, Siegel JH (2015) Tuning of SFOAEs Evoked by Low-Frequency Tones Is Not Compatible with Localized Emission Generation. J Assoc Res Otolaryngol 16(3):317–329. Epub 2015/03/31. https://doi.org/10.1007/s10162-015-0513-0. PubMed PMID: 25813430; PMCID: PMC4417092

53. Charaziak KK, Siegel JH, editors (2015) Low-frequency tone-pip-evoked otoacoustic emissions orginate over a broad cochlear region in chinchillas. Mechanics of Hearing: Proteins to Perception; American Institute of Pysics, Melville NY

54. Ruggero MA (1992) Responses to sound of the basilar membrane of the mammalian cochlea. Curr Opin Neurobiol 2(4):449–456. PubMed PMID: 1525542

55. Whitfield IC, Ross HF (1965) Cochlear-microphonic and summating potentials and the outputs of individual hair-cell generators. J Acoust Soc Am 38:126–131

56. Dewey JB (2022) Cubic and quadratic distortion products in vibrations of the mouse cochlear apex. JASA Express Lett 2(11):114402. Epub 2022/12/02. https://doi.org/10.1121/10.0015244. PubMed PMID: 36456371; PMCID: PMC9704500

57. Wegel R, Lane C (1924) The auditory masking of one pure tone by another and its probable relation to the dynamics of the inner ear. Phys Rev 23:266–285

58. Egan J, Hake H (1950) On the masking pattern of a simple auditory stimulus. J Acoust Soc Am 22:622–630